

# Transition metal silicides and tellurides: Crystal structure, heat capacities, and derived thermodynamic properties from absolute zero to 2200 K

Jane E. Callanan,<sup>a</sup> Ron D. Weir,<sup>a</sup> and Edgar F. Westrum, Jr.<sup>b</sup>

<sup>a</sup> *Department of Chemistry & Chemical Engineering, Royal Military College of Canada, Kingston, Ontario K7K 5L0, Canada.*

<sup>b</sup> *Department of Chemistry, University of Michigan, Ann Arbor, Mi. 48109-1055, U.S.A.*

**Abstract:** The harsh conditions of temperature, pressure, and atmosphere experienced in much of today's technology have fostered the development and detailed study of materials that can withstand these environments and function effectively. The transition metal silicides are stable to high temperatures, retain high tensile strength to these temperatures, resist oxidation, and have low electrical resistivity. They find use as refractory materials, as furnace elements, in high temperature aerospace work, and in interconnect technologies. The transition metal chalcogenides, which also are stable to high temperatures, are layered 2-dimensional solids. As a consequence they exhibit facile cleavage and have highly anisotropic physical properties. They find use as semiconductors, battery components, catalysts, and as solid lubricants at high temperatures. We report here on three materials on which we have made adiabatic calorimetric measurements of heat capacities: tungsten ditelluride  $WTe_2$ , tungsten disilicide  $WSi_{2.06}$ , molybdenum disilicide,  $MoSi_{2.067}$ .

## INTRODUCTION

The demands of modern technology have necessitated the development of new materials that can withstand the harsh conditions of the environment in which they will be used. The most effective and economically viable use of these materials requires thorough characterization of their properties: structural, optical, electrical, and thermodynamic. Complete thermodynamic characterization includes thermochemical properties, e.g., enthalpies, free energies of formation, and thermophysical properties, especially heat capacity, from which entropy, free energy functions, and structural information can be determined. The evaluation of electronic and magnetic contributions to the heat capacity provide further powerful windows on the material.

Adiabatic calorimetry, the preferred method for the determination of heat capacities, is generally available below 450 - 500 K, yet this information may be needed at or above 2000 K. The technical need for use of these materials at very high temperatures requires the determination of properties to these high temperatures. The techniques by which heat-capacity measurements at high temperatures are made present some difficulty as published heat capacities at higher temperatures are derived for the most part from enthalpy increment measurements determined by drop calorimetry, and more recently, by differential scanning calorimetry.

Transition-metal dichalcogenides are especially suitable for engineering uses in hostile environments of extreme temperature and pressure. The general formula  $MX_2$ , where M is a metal from groups IVB, VB, and VIB, and X is a chalcogen. All members of this family crystallize as layered compounds with sheets of metal atoms sandwiched between two sheets of chalcogens. As a result, intralayer bonds are strong but interlayer bonds are weak. These features give rise to facile, horizontal cleavage, marked anisotropy in many physical properties, and to intercalation of foreign atoms. Industrial applications of the dichalcogenides include semiconductors, battery components, catalysts, and high-temperature solid lubricants.

The group 6 silicides also find application as engineering materials. They are refractory materials that are stable at extreme conditions of temperature and pressure, resist oxidation and have high thermal and electrical conductivity. They find use as high-temperature construction materials, for furnace windings and heating elements, as coatings, in interconnect technology, in semiconductors, and in high-temperature aerospace applications. According to the phase diagram, the molybdenum-silicon system shows the existence of three compounds,  $\text{MoSi}_2$ ,  $\text{Mo}_3\text{Si}$ , and  $\text{Mo}_5\text{Si}_3$ . At present, studies of tungsten-silicide and one of the molybdenum disilicides have been completed.

All the materials for which heat capacities are reported in this paper are difficult both to prepare as pure stoichiometric compounds and to analyse; seemingly small deviations from the expected stoichiometry make a significant difference in properties and prevent meaningful comparisons among extant heat capacities. We report here heat capacities and thermodynamic properties of three materials on which we have made adiabatic calorimetric measurements: tungsten disilicide  $\text{WSi}_2$ , tungsten ditelluride  $\text{WTe}_{2.06}$ , molybdenum disilicide,  $\text{MoSi}_{2.067}$ .

## EXPERIMENTAL RESULTS AND DISCUSSION

Tungsten disilicide  $\text{WSi}_2$  (ref. 1) crystallizes at room temperature in a tetragonal  $D_{4h}^{17}$  space group. The molar heat capacity was measured from  $5.9 \leq T/\text{K} \leq 341$ . The heat capacity against temperature curve, shown as  $C_{p,m}/R$  (where  $R$  is the gas constant) in Fig. 1, is smooth and without anomalies.  $S_m^0(\text{cr}, 298.15 \text{ K}) = (68.43 \pm 0.17) \text{ J}\cdot\text{K}^{-1}\cdot\text{mol}^{-1}$  and  $\Delta G_f^0(\text{cr}, 298.15 \text{ K}) = (79.5 \pm 5.5) \text{ kJ}\cdot\text{mol}^{-1}$ .

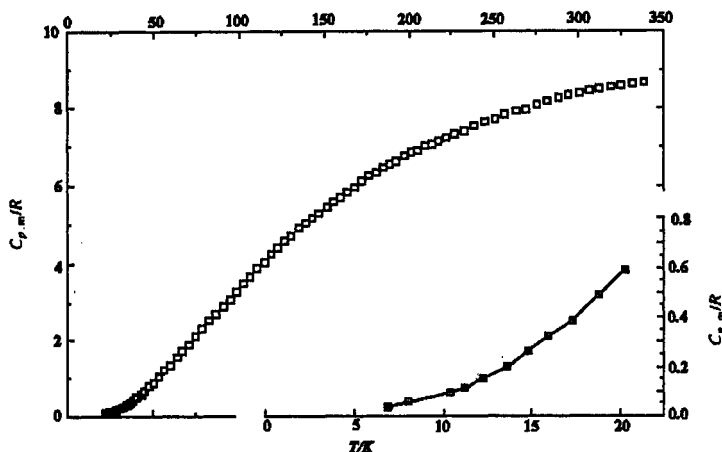


**Figure 1** Experimental molar heat capacities  $C_{p,m}$  at constant pressure plotted against temperature  $T$  for  $\text{WSi}_{2.06}$ . The region below  $T=22 \text{ K}$  is enlarged in the lower right-hand corner.

Figure 2 shows an attempt to extend the heat capacity of  $\text{WSi}_2$  to 1200 K with enthalpy increments determined by the drop calorimetry studies of Mezaki *et al.* (ref. 2) from  $461 \leq (T/\text{K}) \leq 1068$ , and to 2200 K by the drop calorimetric work of Bondarenko *et al.* (ref. 3) at  $1173 \leq (T/\text{K}) \leq 2113$ .

Despite differences in the quality and purity of the sample used, it was reasonable to extend the thermodynamic quantities to 1200 K. Because of the unexpected and unacceptable slope of the heat capacity curve of Bondarenko *et al.* and the consequent fact that the lower temperature heat capacities could not be extended smoothly to the results above 1200 K, no attempt was made to determine properties above 1200 K.

The carefully prepared and analysed sample of tungsten ditelluride  $\text{WTe}_{2.06}$  (ref. 4) used in this study was part of the same sample used for thermochemical studies by O'Hare. (ref. 5) X-ray studies at room temperature showed the structure to be orthorhombic with space group  $D_{4h}^{16}$ . The molar heat capacity was measured from  $5.5 \leq T/\text{K} \leq 329$ ; the heat capacity against temperature curve is shown in Fig. 3 as  $C_{p,m}/R$  (where  $R$  is the gas constant). A broad anomaly is observed between  $92 \leq T/\text{K} \leq 175$ .  $S_m^0(\text{cr}, 298.15 \text{ K}) = (132.70 \pm 0.25) \text{ J}\cdot\text{K}^{-1}\cdot\text{mol}^{-1}$ . A similar but less prominent anomaly can be seen in the heat capacities for  $\text{WSe}_2$ . (ref. 6) These effects are reminiscent of more striking anomalies observed by us in previous studies on

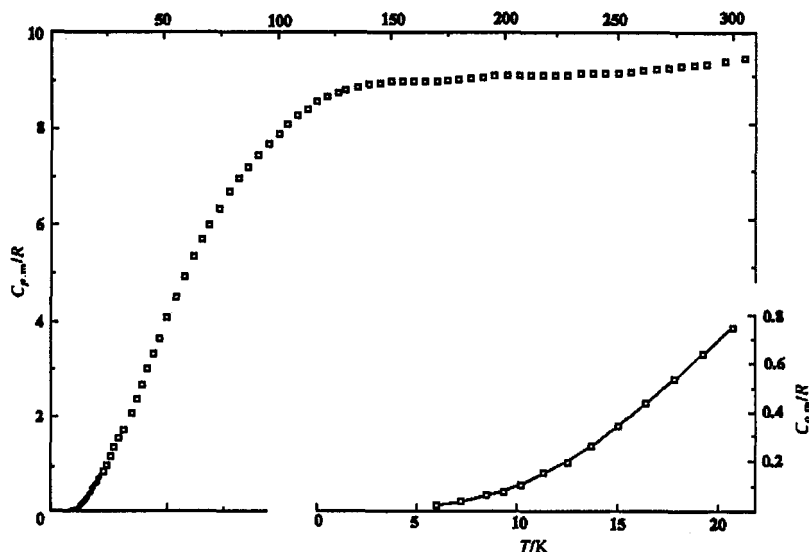


**Figure 2** Experimental molar heat capacities  $C_{p,m}$  at constant pressure plotted against temperature  $T$  for  $WSi_{2.06}$  up to  $T = 2200$  K: a, this work; b, Mezaki et al. (ref. 2); c, Bondarenko et al. (ref. 3).

tetragonal and orthorhombic crystals. (ref. 7-13) In these instances, the anomalies were attributed to highly anisotropic thermal expansivities. No information is available to date on the expansivities or structural changes in the tungsten compounds for the temperature region concerned; however, these materials are known to be highly anisotropic in other properties, e.g., electrical conductivity. (ref. 14) The path of the  $\Theta_D^S$  against temperature curve for  $WTe_2$  indicates a failure of the Debye model to account for our heat capacities and suggests another contribution to the heat capacity. We did observe the existence of an electronic component to the heat capacity in a plot of  $C_{p,m}/T$  against  $T^2$ .

Heat capacities from  $7 \leq T/K \leq 329$  were measured by adiabatic calorimetry on the same sample of  $MoSi_{2.067}$  used for thermochemical measurements. (ref. 15) Room temperature X-ray studies had shown the sample to be tetragonal, of space group  $D_{4h}^{17}$ . The heat capacity against temperature curve, as shown in Fig. 4, was smooth, but showed slight irregularity in the vicinity of  $T = 200$  K. This irregularity is believed to be a consequence of known anisotropy in thermal expansion, resistivity and magnetoresistivity of  $MoSi_2$ . (ref. 16)

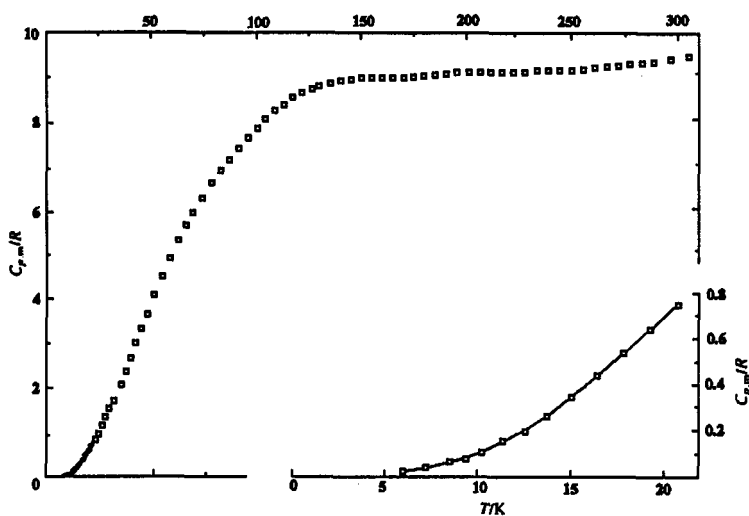


**Figure 3** Experimental molar heat capacities  $C_{p,m}$  at constant pressure plotted against temperature  $T$  for  $WTe_2$ . The region below  $T = 22$  K is enlarged in the lower right hand corner.

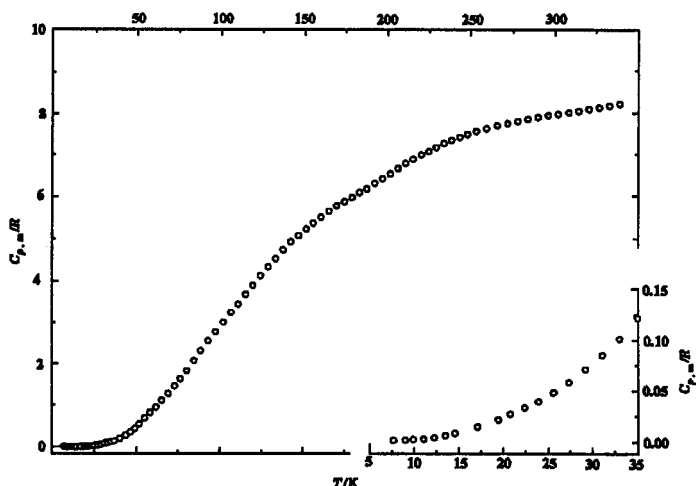


**Figure 4** Experimental molar heat capacities  $C_{p,m}$  at constant pressure plotted against temperature  $T$  for  $WTe_2$ . The region below  $T=22K$  is enlarged in the lower right corner.

Several other investigators had determined the heat capacity of  $MoSi_2$  at temperatures somewhat above those of this study. As Fig. 5 shows, the present work can be extended reasonably to agree with the heat capacities of Douglas and Logan (ref. 17) and of Walker, et al. (ref. 18). The lower temperature measurements of Bondarenko et al. (ref. 19) were made by adiabatic calorimetry and agree reasonably with the others up to  $\sim 800$  K. The measurements of Mezaki (ref. 2) are not included in this figure because the slope was unreasonable for a material in which all degrees of freedom were already believed to be activated. Bondarko et al. (ref. 3) measured enthalpy increments from  $1200 \leq T/K \leq 2200$  by drop calorimetry. Again, the heat capacity against temperature curve had an unreasonable slope; in addition the heat capacity at 1200 K from adiabatic calorimetry was 14 % lower than that obtained at this same temperature from the enthalpy increment work.

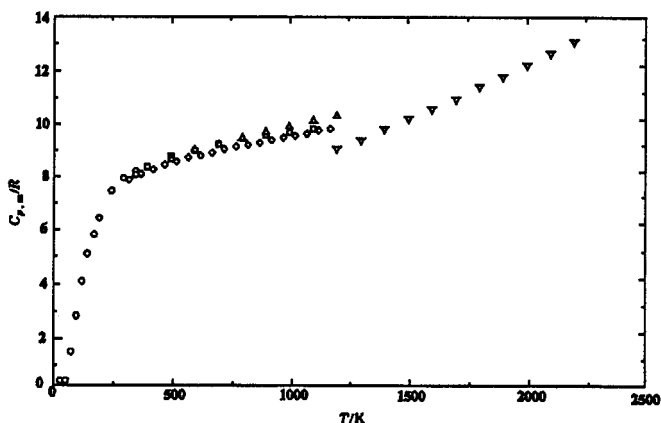


**Figure 5** Molar heat capacity at constant pressure,  $C_{p,m}/R$  of  $MoSi_2$  to  $T = 2200$  K.  $\diamond$ , Douglas and Logan, (Ref. 17);  $\square$ , Walker et al., (Ref. 18);  $\Delta$ , Bondarenko et al., (Ref. 19);  $\nabla$ , Bondarenko et al., (Ref. 3);  $\circ$ , this work.

However, through use of a functional relationship related to the expected course of the high temperature heat capacities and estimated probabilities, we were able to extend the curve reasonably to  $T = 2200$  K, as depicted in Fig. 6. From these results and a very large scale graph, we estimated the  $C_{p,m}/R$  for  $MoSi_2$  to be 10.33.

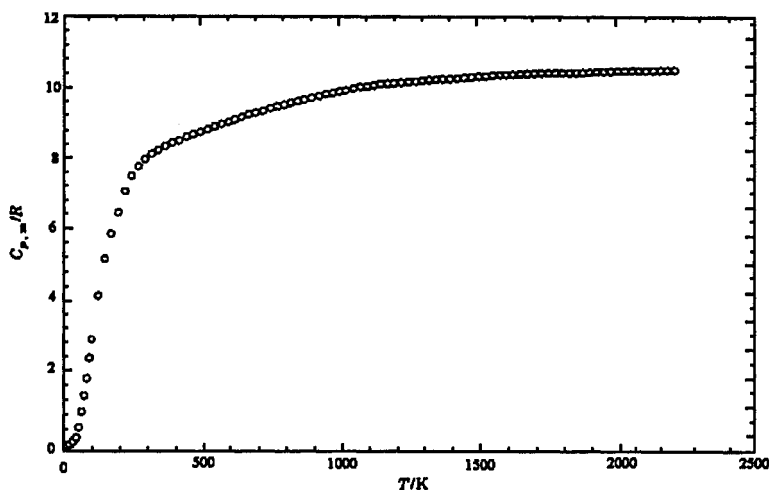


**Figure 6** Estimated molar heat capacity of  $\text{MoSi}_{2,067}$  to 2200 K.

For all three of the substances discussed here an electronic term  $\gamma T$  contributes to the heat capacity. The electronic component is determined from a plot of  $C_{p,m}/T$  against  $T^2$  as  $T \rightarrow 0$  or the more sensitive  $(C_{p,m} - \gamma \cdot T)/T^3$  against  $T^2$ . At very low temperatures it is assumed that  $C_{p,m} = C_v$ . From

$$C_v = \gamma T + aT^3 + bT^5 + \dots \quad \text{and} \quad (1)$$

$$C_v/T = \gamma + aT^2 + bT^4 + \dots \quad (2)$$

the intercept of the  $C_v/T$  plots is  $\gamma$ , the electronic component of the heat capacity. Figures 7, 8, and 9 show the plots for the three compounds reported on here:  $\text{WSi}_2$ ,  $\text{WTe}_2$ , and  $\text{MoSi}_{2,067}$ . The values of  $\gamma$  in table 1 are obtained by multiplying the intercepts indicated on the graphs by the gas constant  $R$ . The  $\gamma$  value obtained by Lasjaunais et al. (ref. 20) from their heat pulse measurements from  $0.2 \leq (T/K) \leq 7$  on  $\text{MoSi}_2$  is shown also in Table 1.

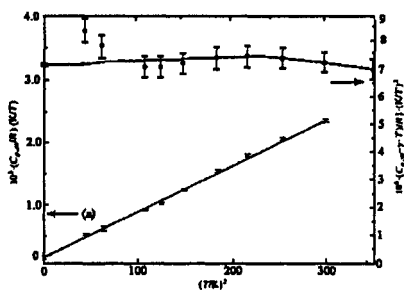


**Figure 7** Plots of a,  $C_{p,m}/RT$  and b,  $(C_{p,m} - \gamma T)/RT^3$  against  $T^2$  for  $\text{WSi}_{2,067}$ . The vertical error bars correspond to a,  $20 (C_{p,m}/R)(K/T)$  and b,  $20 \{(C_{p,m} - \gamma T)/R\}(K/T)^3$ .

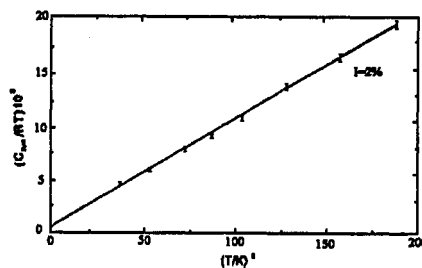


**Figure 8** Plot of  $C_{p,m}/RT$  for  $\text{WTe}_2$  against  $T^2$  for  $\text{WTe}_2$ . Error bars correspond to  $0.02(C_{p,m}/R)(10^3 \cdot K/T)$ .

## CONCLUSIONS

Tungsten disilicide  $\text{WSi}_2$  has no structural phase transition from  $0 \leq T/K \leq 1200$ ; thus, the tetragonal  $D_{4h}^{17}$  remains from  $6 \leq (T/K) \leq 1200$ . It is a stable solid up to 2400 K, melts at  $\approx 2437$  K, and is an excellent engineering material. Tungsten ditelluride has no structural phase transition between  $0 \leq (T/K) \leq 326$ , and thus the orthorhombic space group  $D_{2h}^{16}$  remains over this temperature range. The heat capacity anomaly is believed due to anisotropy, possibly in the electrical conductivity. Heat capacity values are needed at temperatures  $\geq 350$  K. Since molybdenum disilicide has no structural phase transition, it retains the tetragonal  $D_{4h}^{17}$  space group between  $0 \leq (T/K) \leq 2200$ .  $\text{MoSi}_2$  is a stable solid to 2200 K and an excellent engineering material.

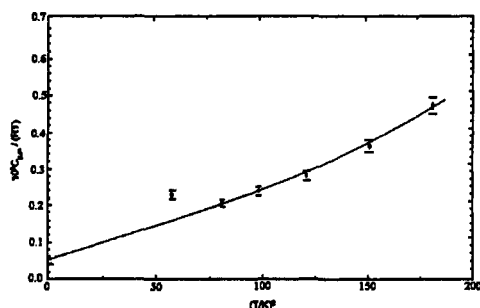


**Figure 9** Plot of  $C_{p,m}/RT$  against  $T^2$  for  $\text{MoSi}_{2,067}$ . Error bars correspond to 0.02 ( $C_{p,m}/R$ ) ( $10^3 \cdot \text{K}/T$ ).

**TABLE 1.** Comparison of  $\gamma$  values.

	$(\gamma/\text{mJ} \cdot \text{K}^{-2} \cdot \text{mol}^{-1})$
Cu	0.744
Al	1.21
W	1.36
Mo	2.11
$\text{MoSi}_{2,067}$	0.54
$\text{MoSi}_2$	0.57 (ref. 20)
WC	0.79
$\text{WSi}_{2,06}$	1.33
$\text{WTe}_2$	5.99

## REFERENCES

1. J. E. Callanan, R. D. Weir, and E. F. Westrum, Jr. *J. Chem. Thermodyn.* **25**, 1391-1401 (1993) and references contained therein.
2. R. Mezaki, E. W. Tilleux, T. F. Jambois, and J. L. Margrave. In *Advances in Thermophysical Properties at Extreme Temperatures and Pressures* (S. Gratch, ed.), pp. 138-144, ASME, New York (1965).
3. V. P. Bondarenko, E. N. Fomichev and A. A. Kalashnik. *Heat Transfer - Soviet Research*, **5**, 76-78 (1973).
4. J. E. Callanan, G. A. Hope, R. D. Weir, and E. F. Westrum, Jr. *J. Chem. Thermodyn.* **24**, 627-638 (1992) and references contained therein.
5. P. A. G. O'Hare, (a) **19**, *J. Chem. Thermodyn.* 675-701 (1987); (b). P. A. G. O'Hare and G.A. Hope. *J. Chem. Thermodyn.* **24**, 639-647 (1992).
6. A. S. Bolgar, Zh. A. Trofima and A. A. Yanaki. *Poroshk. Metall.* **5**, 53-56 (1990).
7. R. D. Weir and L. A. K. Staveley. *J. Chem. Phys.* **73**, 1386-1392 (1980).
8. R. J. C. Brown, J. E. Callanan, R. D. Weir and E. F. Westrum, Jr. *J. Chem. Thermodyn.* **18**, 787-792 (1986).
9. R. J. C. Brown, J. E. Callanan, R. D. Weir and E. F. Westrum, Jr. *J. Chem. Phys.* **85**, 5963-5970 (1986).
10. R. J. C. Brown, J. E. Callanan, T. E. Haslett, R. D. Weir and E. F. Westrum, Jr. *J. Chem. Thermodyn.* **19**, 711-716 (1987).
11. R. J. C. Brown, J. E. Callanan, T. E. Haslett, R. D. Weir and E. F. Westrum, Jr. *J. Chem. Thermodyn.* **19**, 1111-1116 (1987).
12. R. J. C. Brown, J. E. Callanan, R. D. Weir, and E. F. Westrum, Jr. *J. Chem. Thermodyn.* **19**, 1173-1182 (1987).
13. R. J. C. Brown, R. D. Weir, and E. F. Westrum, Jr. *J. Chem. Phys.* **91**, 399-407 (1989).
14. J. P. Troadec, D. Bideau, and E. Guyon. *J. Phys. C: Solid State Physics*. **14**, 4807-4819 (1981).
15. J. E. Callanan, R. D. Weir, and E. F. Westrum, Jr. *J. Chem. Thermodyn.* **28**, O-627 (1996) and references therein.
16. O. Thomas, J. P. Senateur, R. Madar, O. Laborde, and E. Rosencher. *Solid State Commun.* **55**, 629-632 (1985).
17. T. B. Douglas and W. M. Logan. *J. Res. Natl. Bur. Stand. (U. S.)* **53**, 91-93 (1954).
18. B. E. Walker, J. A. Grand and R. R. Miller. *J. Phys Chem.* **60**, 231-233 (1956).
19. V. P. Bondarenko, P. N. B'yugov, V. I. Zmii and A. S. Kuyazhev. *Teplofiz. Vys. Temp.* **10**, 1013 - 1017 (1972).
20. J. C. Lasjaunais, M. Saint-Paul, O. Laborde, O. Thomas, J. P. Senateur and R. Madar. *Phys. Rev. B* **37**, 364-366 (1988).